nature energy

REVIEW ARTICLE

PUBLISHED: 13 JUNE 2016 | ARTICLE NUMBER: 16071 | DOI: 10.1038/NENERGY.2016.71

Promises and challenges of nanomaterials for lithium-based rechargeable batteries

Yongming Sun[1], Nian Liu[1] and Yi Cui[1,2]*

Tremendous progress has been made in the development of lithium-based rechargeable batteries in recent decades. Discoveries of new electrode materials as well as new storage mechanisms have substantially improved battery performance. In particular, nanomaterials design has emerged as a promising solution to tackle many fundamental problems in conventional battery materials. Here we discuss in detail several key issues in batteries, such as electrode volume change, solid–electrolyte interphase formation, electron and ion transport, and electrode atom/molecule movement, and then analyse the advantages presented by nanomaterials design. In addition, we discuss the challenges caused by using nanomaterials in batteries, including undesired parasitic reactions with electrolytes, low volumetric and areal energy density, and high costs from complex multi-step processing, and their possible solutions.

Energy storage is an essential element of the complete landscape of energy processes, closely coupled with energy generation, transmission and usage. Development of lithium-based rechargeable batteries with higher energy density, lower costs and improved safety is highly desirable[1–3]. Over the past 25 years, lithium-ion batteries based on conventional intercalation electrode materials have played a critical role in enabling the widespread availability of consumer electronics and emergence of electrical transportation; however, intercalation-type electrode materials will reach their performance limit in the near future[4]. Significant advancements in battery performance and reductions in cost are expected to come from new battery chemistries, based on different storage mechanisms at the materials level, and different configurations at the cell and system level[5–7]. Among them, alloy-type Si[8–10], Sn[11], P[12,13] and Al[14] anodes, plating- and stripping-type lithium metal anodes[15,16], conversion-type transition metal oxides/sulfides/fluorides/phosphides/nitrides[17–22], and S (Li–S batteries)[23–27] and O_2 (Li–air batteries)[28–30] cathodes are some recent examples demonstrating great promise and broad research interest. While these new electrode materials offer much higher lithium storage capacity, their reaction mechanisms with lithium are significantly different from those of conventional electrodes, resulting in many challenges across multiple length scales, such as: complete destruction of crystal structure; chemical bond breaking/reformation and significant shuffling of host material atoms and molecules; colossal volume change at the particle level; volume change at the electrode and cell level; low electronic conductivity and solid-state lithium diffusivity; and instability of the electrode–electrolyte interface. As such, these problems proved difficult to solve until nanotechnology enabled a materials design paradigm shift from that of conventional battery materials. The emergence and development of nanotechnology in the past three decades has provided new methods and tools to design battery materials on the nanoscale[31–36]. Since the pioneering study of Si nanowires as a battery anode in 2008[8], an exciting research field to exploit nanomaterials design for battery electrodes has emerged to overcome the problems associated with new battery chemistries. A deep understanding of these nanostructured electrode materials has also been obtained, based on advanced nanocharacterization techniques.

Here, we review the field of nanomaterials for energy storage by examining their promise to address the problems of new battery chemistries, as well as the issues associated with nanomaterials themselves. Previous review articles about nanomaterials for lithium-based rechargeable batteries are mostly organized by individual battery chemistries[5,6,37,38]. We believe that different battery chemistries share some common challenges. Thus, instead of examining individual chemistries separately, we organize our Review based on the issues that nanomaterials design can address, including: large volume expansion and fracture; instability of the solid–electrolyte interphase (SEI); electron and ion transport; and host atom and molecule diffusion in batteries. We use examples from various battery chemistries to illustrate these fundamental nanomaterials design principles. In addition, we also address various challenges for nanomaterials, including significant side reactions with electrolytes due to the high electrode/electrolyte contact area, limited volumetric energy density of the entire electrode due to low mass loading and tap density, and high cost due to complex nanomaterials synthesis, and discuss how these challenges might be addressed.

Cracking and fracture of particles and electrodes

Traditional intercalation-type electrode materials undergo negligible or small volume changes (<10%) during the lithium insertion/extraction processes, whereas new high-capacity electrode materials usually have massive volume changes due to their intake of large amounts of lithium. The large volume change during the charge/discharge process has been identified as one of the major issues preventing the application of high-capacity electrode materials since the late 1990s[39]. For example, the volume expansions of alloy-type anodes are as high as 420% for Si, 260% for Ge and Sn, and 300% for P, all much larger than 10% for traditional graphite anodes. For lithium metal anodes, owing to their 'hostless' nature, the relative volume change is virtually infinite. These dramatic volume changes induce mechanical degradation of both the active materials and electrodes during electrochemical cycling, significantly shortening the cycle life.

One well-known example is the Si anode, which exhibits very large volume fluctuations. Significant structure changes of Si occur during the initial lithiation and delithiation processes. Upon the

[1]Department of Materials Science and Engineering, Stanford University, Stanford, California 94305, USA. [2]Stanford Institute for Materials and Energy Sciences, SLAC National Accelerator Laboratory, 2575 Sand Hill Road, Menlo Park, California 94025, USA. *e-mail: yicui@stanford.edu

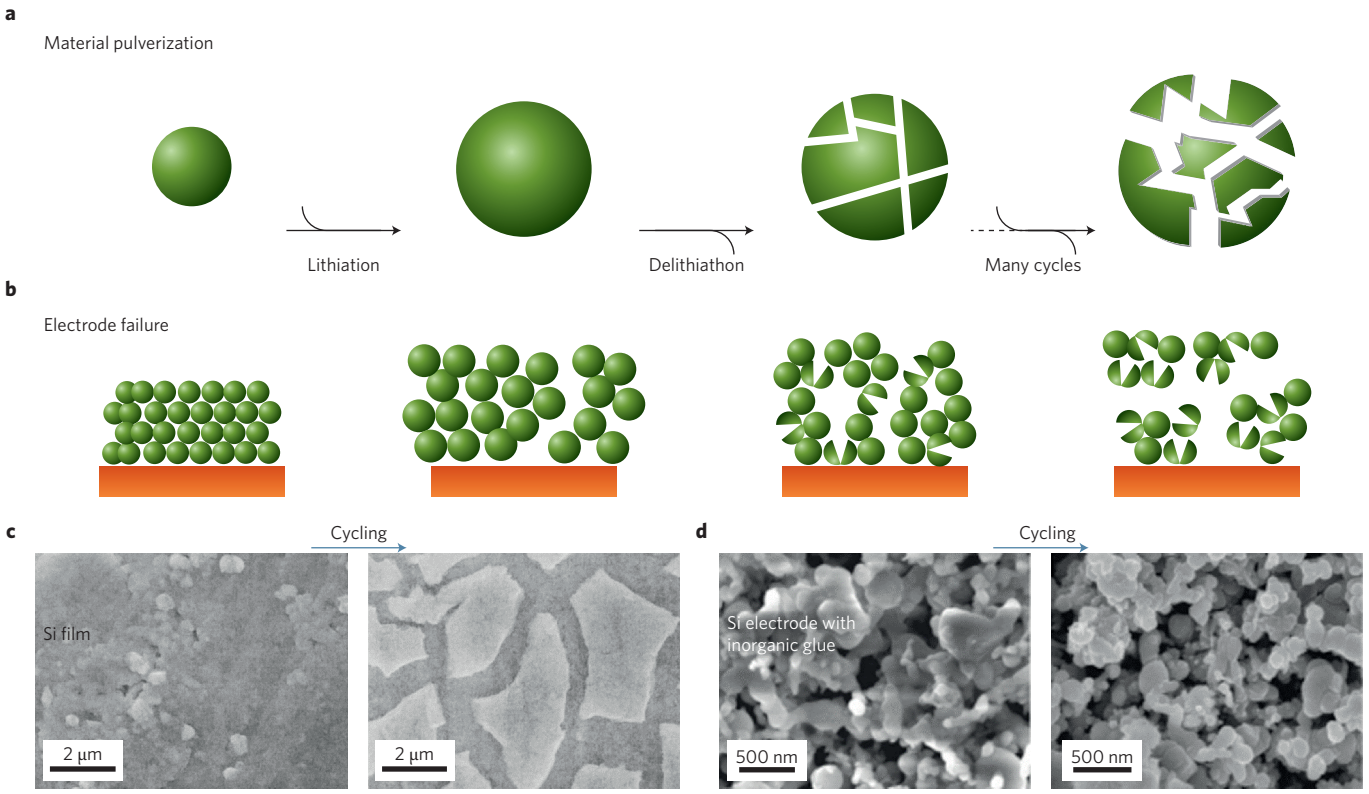

Figure 1 | Cracking and fracture of high-capacity active particles and electrodes over lithiation/delithiation cycling. a,**b**, The mechanical degradation of high-capacity material at the particle level (**a**) and electrode level (**b**) during discharge/charge cycling. **c**, SEM images of a deposited 250 nm Si film on Cu before (left) and after (right) 30 discharge/charge cycles between 1.2 and 0.02 V at 2.5 C. **d**, SEM images of a Si nanoparticle electrode before (left) and after (right) 20 discharge/charge cycles between 0.9 and 0.01 V at C/10. The Si film electrode cracked like mud in a dry lake bed bottom. The morphology of the Si nanoparticle electrode did not change much due to limited particle and electrode fracture. Figures reproduced from: **c**, ref. 44, ECS; **d**, ref. 49, ECS.

first lithiation process, crystalline Si changes to amorphous Li_xSi, with anisotropic volume expansion[40–42]. Similar to Si anodes, other alloy-type anodes, conversion-type anodes/cathodes and sulfur cathodes also undergo dramatic structural transformations and large volume changes during their charge and discharge processes. For conversion-type electrodes, the products from the first lithiation process are ultra-fine metal nanoparticles (for example, 2 nm) embedded in a binary lithium compound (for example, Li_2O, Li_2S, LiF, Li_3P or Li_3N) matrix[17,19,43]. After delithiation, the volume of these high-capacity electrode materials shrinks. Such inherently large volumetric expansion and contraction causes cracking, fracture and pulverization of active particles on cycling, leading to loss of electrical contact (Fig. 1a).

Besides the particle-level fracture, significant mechanical degradation occurs at the electrode level through displacement over layers of particles across the electrode. The repeated expansion and contraction of particles leads to their detachment from surrounding electrical connections and delamination from the electrode (Fig. 1b). This mechanism of cracking, fracture and pulverization of particles and electrodes eventually leads to dramatic capacity decay for most of the bulk films[41,44] and large particles (Fig. 1c).

One of the essential advantages of nanomaterials is their ability to resist mechanical degradation at the particle and/or electrode levels[45]. The critical fracture size — one of the fundamental parameters for high-capacity electrode materials — depends on reaction type (for example, alloying reactions and conversion reactions), mechanical properties, crystallinity, density, geometry and volume expansion ratio of the nanomaterial. Moreover, electrochemical reaction rates play a crucial role in cracking and fracture of particles, as larger stresses can occur at faster charging/discharging rates. With particle sizes below the critical size, the lithiation-induced strain can be accommodated without inducing particle cracking or fracture. The mechanism of stress generation, cracking and fracture of particles, and size dependence of Si have been systematically investigated by calculations[46], *in situ* atomic force microscopy[41], scanning electron microscopy (SEM)[42], transmission electron microscopy (TEM) and *in situ* TEM[47,48]. The critical fracture sizes of crystalline Si nanopillars and nanowires are 240–360 nm and 300–400 nm, respectively, depending on the electrochemical reaction rate[42], whereas that of crystalline Si particles is smaller (~150 nm)[48].

Particle-level fracture can be solved by using various nanostructures below the critical breaking size apart from nanopillars and nanoparticles, such as nanowires, nanotubes, nanorods and nanocomposites. Electrode-level fracture, however, is another challenge, owing to the accumulation effect of numerous particles. Traditional electrodes consist of active particles, carbon black and polyvinylidene fluoride binder. The expansion of particles leads to an increase in electrode volume, whereas their contraction results in the shrinkage of the entire electrode. Such repetitive volume changes eventually lead to the mechanical failure of electrodes and their fast capacity fading due to electrical disconnection and physical delamination of the active material. Thus, it is highly desirable to maintain the electrical connection of active particles to the current collector and suppress the cracking and fracture of electrodes over many discharge/charge cycles. Using amorphous Si as an inorganic glue to bind Si nanoparticles onto the current collector can solve the issue of electrical contact in conventional electrode fabrication routes, and limits particle and electrode failure (Fig. 1d)[49]. Among various other techniques, the use of robust polymeric binders (for example, an alginate binder[50], a cross-linked binder comprising cyclic and linear polymers[51], and a catechol-conjugated polymer binder[52]) is a promising method to mitigate the large volume expansion and

inhibit mechanical fracture of silicon electrodes during cycling. Additionally, an active–inactive nanocomposite was first designed by Dahn to reduce the negative effects associated with the large volume change of high-capacity electrode materials[53]. The volume expansion stresses of Si can be mitigated through nanoscale architectures of Si/metal nitride and Si/metal carbide composites[54,55].

Sulfur is one of the most promising cathode materials for rechargeable lithium batteries owing to its high specific capacity and low cost. Theoretically, the volume expansion of sulfur is as large as 80% when it is fully converted to Li_2S on lithiation. Thus, sulfur cathodes suffer from the same issue of pulverization as most other high-capacity electrode materials. Compounding the problem, the lithiation process of sulfur involves various soluble polysulfide intermediates. The expansion of the sulfur cathode on lithiation will lead to leaking of these soluble polysulfide intermediates from the electrodes, causing decay of the battery performance[7]. Some early work has shown that nanostructures of carbon materials, metal oxides and polymers have sulfur- and/or polysulfide-adsorbing effects, which appreciably improve the electrochemical performance of sulfur cathodes[56–58]. It is common knowledge that an encapsulation or coating layer can help to trap these soluble intermediates within the sulfur cathode (discussed below). Efforts to trap sulfur have been mainly focused on the use of porous carbons, via fusing the sulfur into their structure[23,59], or encapsulating sulfur particles or sulfur/carbon composites with various protective layers[24,60–62]. Nazar and co-workers pioneered the encapsulation of sulfur within the channels of mesoporous carbon[23]. The strategy of adjusting the amount of sulfur infusion into mesoporous carbon to leave space for volume expansion to occur has been demonstrated, although it may face the difficulty of uniform sulfur filling[23]. Alternatively, by using various protective layers to form core–shell or yolk–shell nanostructures, the electrochemical performance of sulfur cathodes can be improved. For a full-filled core–shell structure, expansion of the sulfur core could cause the protective shell layer to crack and fracture, resulting in leakage of the intermediate polysulfides. The critical problem of volume expansion has been successfully solved by the construction of yolk–shell nanostructures with designed void space. Of notable mention are the very recent works on S–TiO_2 yolk–shell nanoarchitectures[63] and polymer-encapsulated hollow sulfur nanospheres[25,64]. Owing to the presence of internal void space inside the shell, the volume expansion of sulfur on lithiation can be fully accommodated, allowing these yolk–shell nanostructures to deliver much improved long-term cycling performance. In particular, as Li_2S is already in the fully lithiated and fully expanded state of sulfur, using Li_2S nanoparticles as the starting material can circumvent the problem of particle cracking and fracture induced by volume expansion, and minimize mechanical degradation at the electrode level[65].

Solid–electrolyte interphase

The electrochemical working potentials of anode materials are below the reduction potential of organic carbonates commonly employed in lithium-based battery electrolytes (around ~1 V[66]; potentials are versus Li^+/Li^0.). During battery charging, electrochemical reduction of the electrolyte occurs and produces a passivating SEI layer on the anode surface. The SEI is a lithium-ion conductor but an electronic insulator, leading to the termination of SEI growth at a certain thickness[67]. A stable SEI layer allows for high Coulombic efficiency and the long-term stability of anodes benefiting from the surface passivation. However, owing to repetitive large volume changes on lithiation and delithiation[41], the electrode/electrolyte interface moves and changes significantly, making it very challenging to maintain a stable SEI for high-capacity electrode materials.

As shown in Fig. 2a,b, solid and hollow Si structures expand towards the electrolyte on lithiation and contract during delithiation[68]. The SEI breaks due to the large volume changes, thus exposing electrode surface to electrolyte and inducing the growth of new SEI (Fig. 2a,b). This accumulated SEI over cycling decays the battery performance for the following reasons: first, electrolyte and lithium are consumed during the continuous SEI formation; second, a thick SEI layer leads to a long lithium-ion diffusion distance; and finally, mechanical stress from a thick SEI layer causes material degradation.

Nanotechnology provides new methods to overcome the unstable SEI formation to achieve reversible cycling and long cycle life for high-capacity anode materials. Taking Si anodes as an example, our group has pioneered the construction of encapsulating nanostructures with an electrolyte blocking layer and a pre-defined void space to counteract the issue of volume expansion and achieve stable SEI for high-capacity electrode materials[68–71]. As shown in Fig. 2c, Si–SiO_x double-walled nanotubes have a static SiO_x interface with the electrolyte and form a stable SEI layer after the formation cycles. The inner Si surface moves back and forth during the lithiation and delithiation processes but does not break the shell structure and contact the electrolyte[68]. Stable cycling for 6,000 cycles was demonstrated in half cells. Other successful examples for stable SEI formation include encapsulating Si nanoparticles in hollow carbon tubes (Fig. 2d)[71] and Si–C yolk–shell nanoparticles[69]. Moreover, the strategy of engineering encapsulation nanostructures is also generally applicable for other high-capacity electrode materials with large volume changes, such as alloy-type tin (Fig. 2e)[72] and conversion oxides (Fig. 2f)[73]. Very recently, Al–TiO_2 yolk–shell nanoparticles with tunable interspace were successfully synthesized and showed well-maintained structure for 500 charge/discharge cycles (Fig. 2g)[14]. All the above-mentioned encapsulation nanostructures with an inner void space exhibit long electrochemical charge/discharge cycling lifetimes, indicating that a stable SEI layer is successfully formed on the outer surface of these nanostructures.

Lithium metal holds the highest possible energy density as an anode for rechargeable lithium batteries. In particular, it is the ultimate anode choice for high-energy Li–S and Li–air batteries. However, lithium metal has virtually infinite relative volume expansion during charging. Thus, the challenge of stabilizing the SEI of lithium metal anodes is even greater than that of Si anodes. Figure 3a illustrates the SEI breaking and reformation during lithium metal plating/stripping, which leads to rapid consumption of electrolyte, loss of lithium and low Coulombic efficiency[74]. A promising strategy to tackle the unstable SEI issue is to engineer a chemically stable and mechanically robust nanostructured interfacial layer between the lithium metal anode and the electrolyte, such as a layer of interconnected hollow carbon nanospheres[15] or ultrathin BN/graphene[75]. It is observed that lithium metal deposition happens underneath a monolayer of hollow carbon nanospheres on the metal current collector, while a stable SEI forms on the outer surface of the carbon nanosphere layer. The SEI, together with the hollow nanosphere layer, moves up and down during cycling without forming new SEI (Fig. 3b)[15]. An additional challenge of the lithium metal anode — namely the growth of lithium dendrites across the electrode surface caused by non-uniform electrodeposition — can be solved by this protective coating (Fig. 3c)[15]. Construction of a stable artificial SEI layer for the lithium metal anode before cycling is another promising strategy[76,77]. A uniform Li_3PO_4 SEI layer can be formed *in situ* on the lithium metal surface via the reaction of polyphosphoric acid with lithium metal and its native film (Fig. 3d)[77]. The artificial SEI can restrain the unfavourable reaction between the lithium metal and the electrolyte, and suppress the growth of lithium dendrites. Meanwhile, a stable and uniform SEI layer can also be formed on the lithium metal surface by using various electrolyte additives (Fig. 3e)[78]. When both lithium polysulfide and lithium nitrate were used as additives in ether-based electrolyte, the electrolyte decomposition was minimized and the growth of lithium dendrites was significantly suppressed.

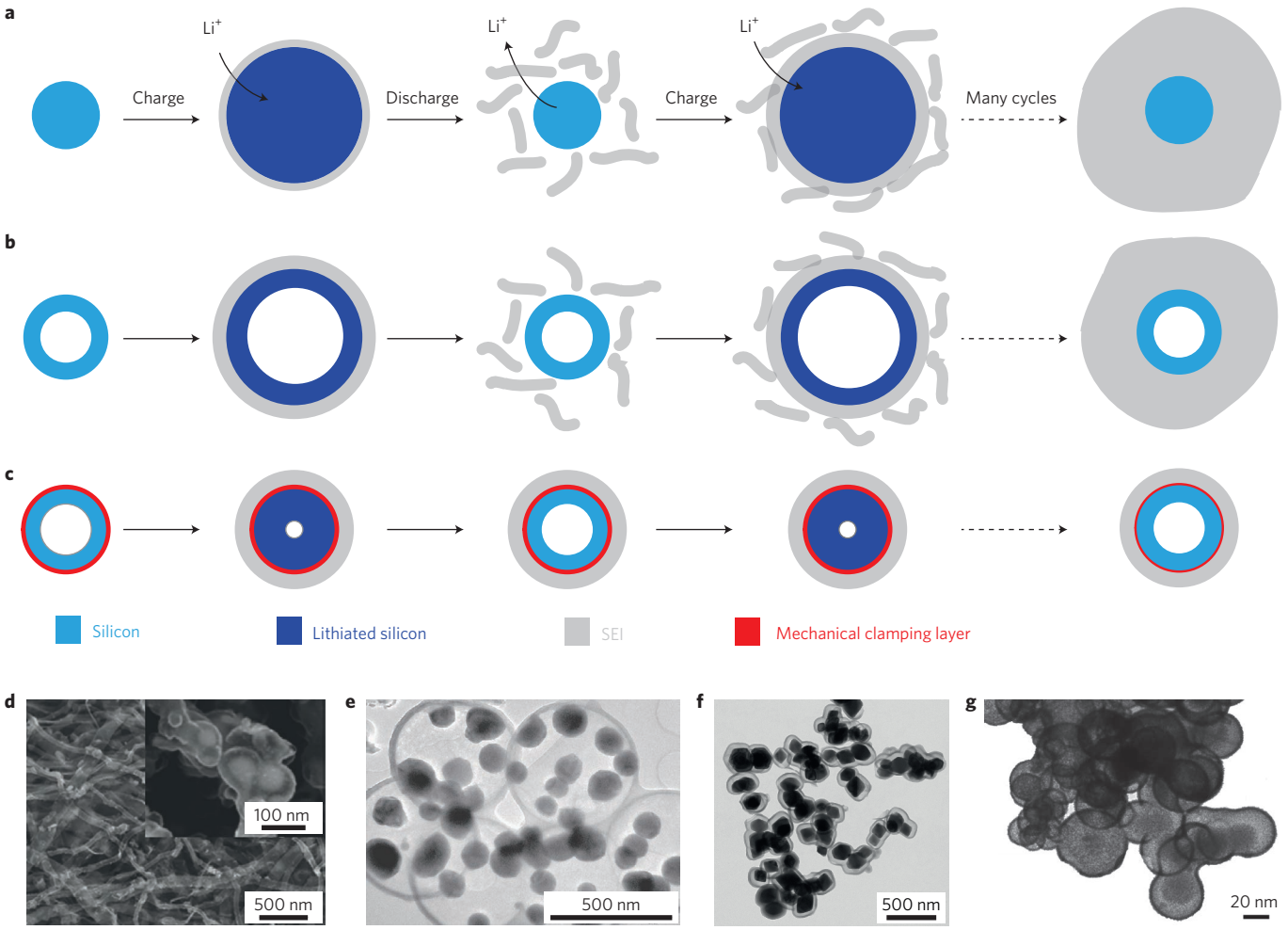

Figure 2 | SEI formation on a silicon surface and various encapsulated nanostructures for stabilizing the SEI. a,**b**, Schematic of a varying and unstable SEI layer built outside a solid silicon nanowire (**a**) and nanotube (**b**). **c**, Schematic of a thin and stable SEI built on a hollow silicon nanotube with a mechanical constraining layer. **d**–**g**, SEM/TEM images of encapsulated nanostructures with an electrolyte-blocking layer and a pre-defined void space: encapsulating Si nanoparticles in hollow carbon nanotubes (**d**), Sn–C (**e**) and FeO_x–C yolk–shell nanoparticles (**f**), and Al–TiO_2 yolk–shell nanoparticles (**g**). Figures reproduced from: **a**–**c**, ref. 68, NPG; **d**, ref. 71, ACS; **e**, ref. 72, Wiley; **f**, ref. 73, Wiley; **g**, ref. 14, NPG.

Electron/ion transport

Fast charge carrier transport inside individual particles and at the whole electrode is crucial to battery performance. Highly conductive pathways for electrons and short transport distances for ions can help to achieve good rate capability and to activate insulating electrode materials. Compared with micrometre-scale materials, nanomaterials possess much smaller dimensions. For individual particles, lithium-ion insertion/extraction and electron transport within the nanoparticles are significantly enhanced due to the short transport distances compared with those of microparticles[5]. Coating active particles with a conductive layer and embedding active particles in a conductive matrix are general routes to improve the electron conductivity for individual particles. For example, core–shell Si–C nanofibres were developed and showed excellent rate capability[79]. Within the structure, the well-defined one-dimensional (1D) electronic pathways facilitate efficient electronic conduction, while the small diameter of the electrospun fibres enables short transport distances for lithium-ion diffusion[79]. Another example of a nanostructured alloy-type anode demonstrating fast charge carrier transport is a Sn/C composite with uniformly dispersed Sn nanoparticles (10 nm) in a spherical carbon matrix. It provided ~600 mAh g^{-1} even at a high rate of 20 C due to the continuous transport path for lithium ions and electrons inside the Sn/C composite spheres[80]. Besides amorphous carbon materials, other conductive materials were also used to enable fast charge carrier transport for battery materials. High rate capability and high areal capacity were realized for a Li_2S cathode encapsulated with a shell of conductive metal sulfides[65]. Excellent rate capability was also achieved for graphene-based nanocomposites (for example, a P/graphene composite anode)[13].

Besides the rapid electron and ion transport at the particle level, it is very important to realize rapid transport at the electrode level, which is crucial for the high mass loading of practical batteries. A few strategies have been developed to achieve fast electron/ion transport inside an electrode. First, a general strategy is to construct nanostructured active materials on metal current collectors, such as self-supported nanowire arrays[8,81], interconnected hollow nanospheres[82] and inverse opal nanostructures[83]. Second, much effort has been devoted towards deposition of active materials on nanoarchitectured metal current collectors (for example, Cu nanopillar[20] and nanocable arrays[84] on Cu foils). Additionally, the strategy of depositing active materials on 3D conductive networks to make free-standing electrodes, such as carbon nanotube sponge-based 3D electrodes[85] and graphene foam-based 3D electrodes[86], has been successfully used for various electrode materials to achieve high rate capabilities.

Configuring electrodes with the direct growth of self-supported active materials on metal current collectors has been confirmed as an

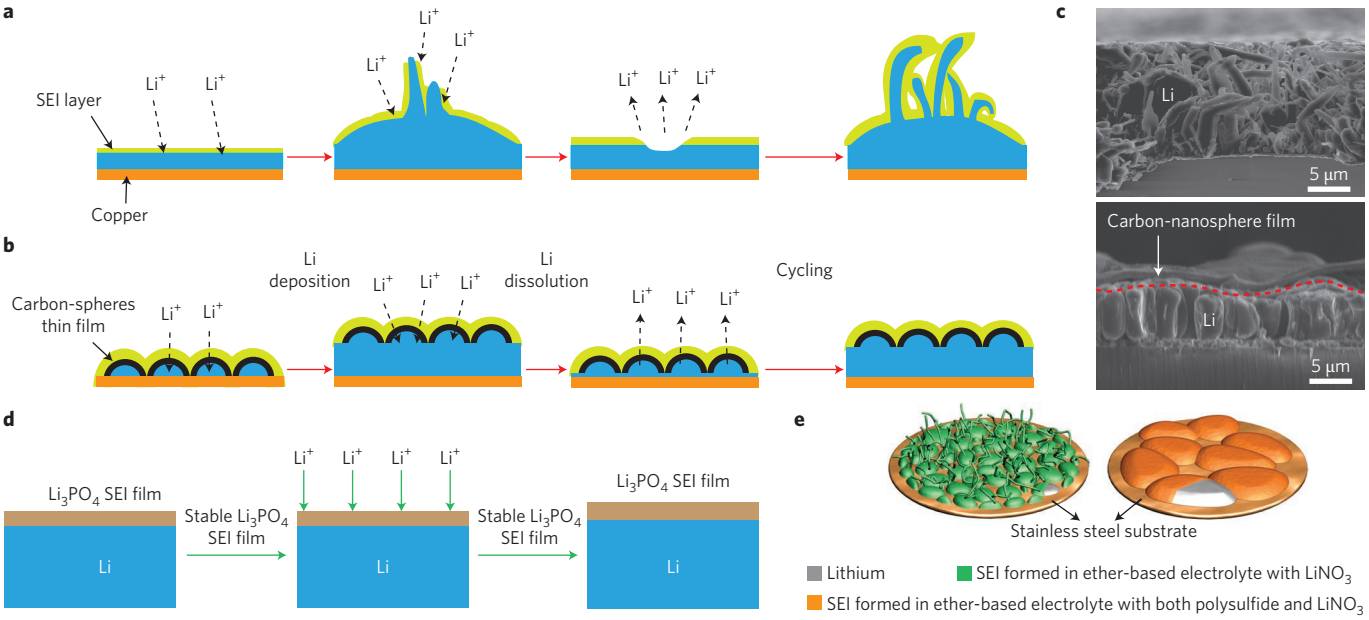

Figure 3 | SEI formation on a lithium metal surface and various solutions for stabilizing the SEI. a, Schematic of the continuous breaking and growth of the SEI layer (yellow) on the surface of deposited lithium (blue). **b**, Schematic of stabilizing the SEI layer by covering the Cu substrate with a hollow carbon nanosphere layer. **c**, SEM cross-section images of the deposited lithium metal on Cu substrates without (top) and with (down) a hollow carbon nanosphere layer. **d**, Schematics of the Li_3PO_4-modified Li metal anodes during SEI formation and cycling. **e**, Schematic illustration showing the morphology difference of lithium deposited on the stainless steel substrate in the two electrolytes (both contain lithium nitrate) without (left) and with (right) lithium polysulfide. Figures reproduced from: **a**–**c**, ref. 15, NPG; **d**, ref. 77, Wiley; **e**, ref. 78, NPG.

effective route to achieve fast electron/ion transport. Typical examples are the construction of alloy-type Si and Ge nanowires on stainless steel current collectors (Fig. 4a)[8,87] and conversion-type Co_3O_4 nanowires on a Ti foil[81]. The Si nanowires are electrically connected to the metal current collector, enabling robust electrical contact during the charge and discharge cycling. The continuous 1D nanowire structure allows for fast electron transport, while the small diameter of these nanowires enables fast ion diffusion rates. Thus, high charge transport rates can be achieved at the electrode level. Moreover, the geometry of nanowire arrays on a current collector also has the benefit of alleviating cracking and fracture issues that afflict films and electrodes composed of bulk particles. Other nanoarchitectures on metal current collectors, such as Si anodes with interconnected hollow nanospheres[82] (Fig. 4b) and TiO_2–sulfur cathodes with inverse opal structures[83], have also achieved fast charge transport. The 3D hollow nanospheres and inverse opal nanostructures increase the accessible surface area to the electrolyte, allowing fast lithium-ion transport to and from the active material. Moreover, these 3D interconnected nanostructures are directly connected to the current collectors, maintaining good electrical contact during the lithiation and delithiation processes. In addition, the discussed nanoarchitectures on metal current collectors provide buffer space for any volume expansion during the lithiation process and thus suppress the mechanical degradation of electrodes.

Direct manipulation and engineering of the nanoarchitectures of metal current collectors and the deposition of active nanomaterials have also been demonstrated to realize 3D electrodes with high electron/ion transport rates. Among the literature, the self-supported Fe_3O_4/Cu nanoarchitectured electrode is very typical[20]. Its fabrication involves the growth of 3D arrays of Cu nanopillars onto a Cu foil by electrodeposition, followed by the further electrodeposition of polycrystalline Fe_3O_4 on these Cu nanopillars (Fig. 4c). Additionally, conductive nanostructured scaffolds (for example, 3D porous Cu layers[88] and graphene frameworks[89]) on Cu foils can render low local current density to suppress the growth of lithium dendrites due to the porous skeleton and high electroactive surface area with fast electron/ion transport rates, enabling a high-performance lithium metal anode (Fig. 4d,e).

Besides the various strategies for constructing nanoarchitectures on metal current collectors, the preparation of free-standing conductive 3D networks in lieu of using metal current collectors provides another route to achieve fast charge transport at the electrode level. In our previous work, a Si–C nanotube coaxial sponge was successfully developed as a binder-free anode for lithium-ion batteries, where amorphous Si was deposited on an interconnected carbon nanotube network (sponge, Fig. 4f)[85]. The highly conductive carbon nanotube cores work as efficient electron transport pathways along the 1D direction, while the interconnected network renders the whole electrode highly electrically conductive. Such features afford very large areal mass loading (8 mg cm^{-2} Si) to the electrode and thus enable a high areal capacity.

Long-distance electrode atom/molecule movement

Traditional insertion-type electrode materials are stable hosts. They do not undergo bond breaking and exhibit only minor structure changes and small volume expansion (<10%) on lithium insertion/extraction. High-capacity electrode materials, in contrast, undergo significant bond breaking and complete crystallographic structure changes followed by structural degradation. Therefore, their use in lithium-based rechargeable batteries has traditionally been regarded as impossible. These high-capacity electrode materials face serious challenges of active atom/molecule diffusion during the repeated charge and discharge processes due to the large structure change or even phase change between solid, liquid and gas, causing critical issues related to battery performances. In general, there are three kinds of electrode atom/molecule movement: (1) phase change and the related atom/molecule diffusion, such as solid–liquid phase transformation for the sulfur cathode in Li–S batteries (Fig. 5a) and gas–solid–liquid phase transformation for the O_2 cathode in Li–O_2 batteries; (2) the growth of lithium dendrites during electrochemical Li plating in secondary Li metal batteries (Fig. 5b); and (3) large volumetric expansion due to the

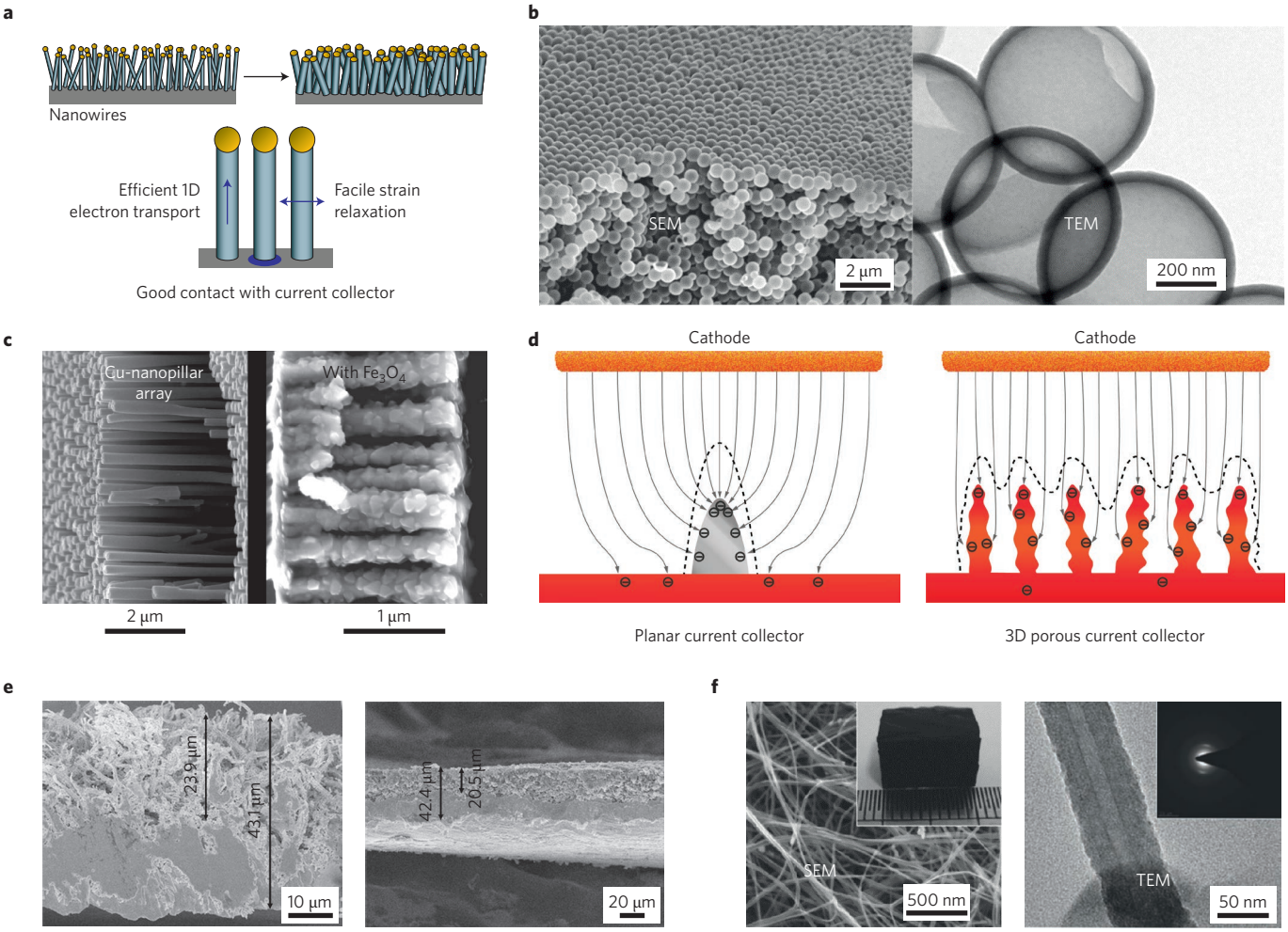

Figure 4 | Construction of nanostructured high-capacity electrodes with fast electron and ion transport rates. a, Nanowires electrodes grown directly on the current collector with fast electron and ion transport rate, good electrical connectivity and free space for volume expansion. **b**, SEM (side view 45° tilt, left) and TEM (right) images of the electrode comprising 3D interconnected hollow Si nanospheres. **c**, Cross-sectional views of a Cu-nanostructured current collector before (left) and after (right) Fe_3O_4 deposits. **d**, Illustration of the electrochemical deposition processes of lithium metal on a planar current collector and 3D current collector. **e**, Spatial distribution of a lithium metal anode in a 3D Cu current collector before (left) and after (right) lithium deposition. **f**, SEM image of a 3D porous carbon nanotube sponge (left) and TEM image of a Si–C nanotube sponge (right). Figures reproduced from: **a**, ref. 8, NPG; **b**, ref. 82, ACS; **c**, ref. 20, NPG; **d**–**e**, ref. 88, NPG; **f**, ref. 85, Wiley.

intake of large amounts of lithium for high-capacity alloy-type and conversion-type electrodes (Fig. 5c).

The sulfur cathode is a typical example of an electrode system that faces a serious challenge with molecule movement due to the formation of intermediate polysulfides during the discharge process. The dissolution of polysulfide intermediates into the electrolyte is one of the key obstacles deterring a long cycle life for Li–S batteries[23]. Upon the discharge process, solid sulfur cathodes go through a series of soluble polysulfide intermediates (Li_2S_n, $4 \leq n \leq 8$) and become insoluble Li_2S_2 and Li_2S that precipitate out at the cathode (Fig. 5a). The as-formed Li_2S_2 and Li_2S are converted back to sulfur via soluble polysulfide intermediates during the charge process[90]. The dissolution and precipitation of the active materials during the charge and discharge processes alters the morphology, reduces the surface conductivity of the electrode, induces strain inside the electrode and hence degrades the cycling stability of Li–S batteries[91]. Moreover, the dissolution of these intermediates into the electrolyte leads to the shuttle effect, which decreases the active mass utilization and leads to low Coulombic efficiency[7].

To date, extensive research has been conducted with a focus on engineering the material and/or electrode structure to effectively trap soluble polysulfides through physical and chemical means. Nanostructures provide new merits and opportunities to design better electrodes and are shown to be one of the most effective ways to understand and address the polysulfide diffusion problem in Li–S batteries. As discussed in 'Cracking and fracture of particles and electrodes', the physical encapsulation of sulfur within the channels of mesoporous carbon and construction of yolk–shell nanostructures with designed void space are successful methods to solve the volume expansion challenge of sulfur electrodes. During the discharge process, sulfur reacts with lithium to form Li_2S via soluble polysulfide intermediates accompanied by volume expansion. The soluble polysulfide intermediates cannot leak out easily during the discharge process due to the physical barrier (Fig. 5d).

Apart from the physical trapping of dissolved polysulfides, the chemical confinement of these intermediate polysulfides can play an important role in suppressing their diffusion away from the cathode. Understanding the interfacial properties of sulfur, lithium sulfide and intermediate polysulfides between the trapping/protecting/adsorption materials is crucial for further improvement of battery performance. In our studies, the preferred deposition of polysulfides on the tin-doped indium oxide (ITO) surface during charge/discharge cycling was confirmed by a model system of a polysulfide–ITO micropatterned glassy carbon cathode. Based

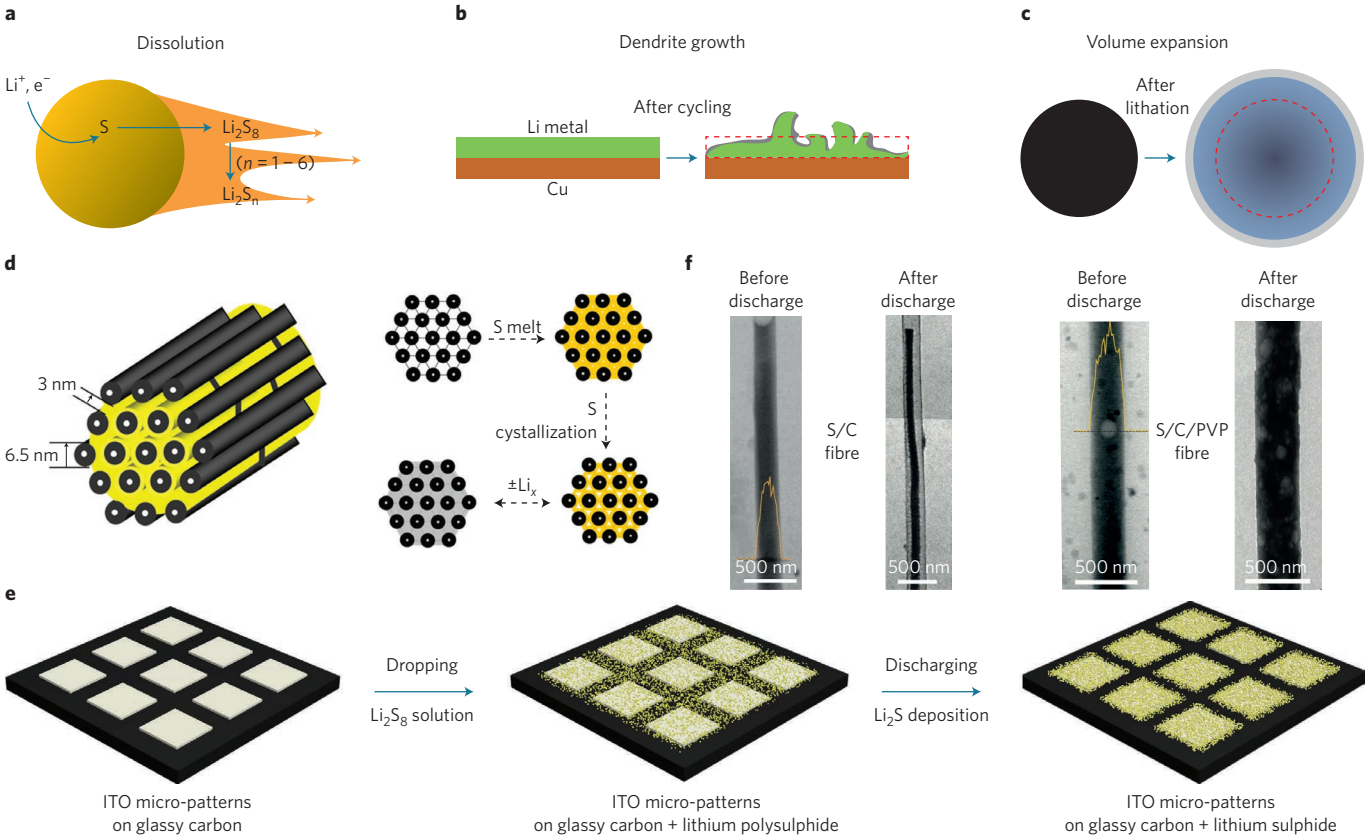

Figure 5 | Understanding of and solutions for the electrode atom/molecule movement. a–c, Schematic of electrode atom/molecule movement in different electrode systems: polysulfide dissolution and diffusion for sulfur cathodes (**a**), lithium dendrite growth for lithium metal anodes (**b**) and volume expansion for alloy and conversion-type electrodes (**c**). **d–f**, Solutions for the polysulfide diffusion for sulfur cathodes. A schematic diagram of the sulfur (yellow) confined in the interconnected pore structure of mesoporous carbon, CMK-3, formed from carbon tubes that are propped apart by carbon nanofibres (**d**). Schematic of the fabrication of a polysulfide–ITO micropattern glassy carbon cathode to show the nature of polysulfide deposition (**e**). TEM image of the sulfur-encapsulated carbon nanofibres without (left) and with (right) polymer functionalization. The yellow line represents the energy-dispersive X-ray spectroscopy counts of the sulfur signal along the dashed line (**f**). Figures reproduced from: **d**, ref. 23, NPG; **e**, ref. 92, NPG; **f**, ref. 61, ACS.

on this understanding, an ITO pattern was introduced onto the sulfur/carbon nanofibre electrode, and much improved electrochemical performance was achieved via such spatially controlled polysulfide deposition (Fig. 5e)[92]. Moreover, the structure changes of sulfur encapsulated by hollow carbon nanofibres before and after the discharge operation were investigated by TEM. After discharge, the lithiated sulfide product detached from the carbon surface due to the low bonding energy between them, leading to the loss of electrical contact and the degradation of electrochemical performance. Such a problem was solved by modifying the interface between the carbon and sulfur with an amphiphilic polymer (polyvinylpyrrolidone, PVP), which bonds strongly with both the carbon surface and Li_xS clusters (Fig. 5f)[61]. Besides ITO and PVP, many other conductive polymers[60], oxides[93] and sulfides[65] show chemical bonding with the polysulfide species, which is favourable for restraining their diffusion. Among three well-known conductive polymers, poly(3,4-ethylenedioxythiophene) (PEDOT), polyaniline and polypyrrole, PEDOT exhibited the best confinement effect on polysulfide dissolution[60]. Some examples, demonstrating the combined effects of physical and chemical confinement of intermediate polysulfides, include a layer of polymer coating on the carbon/sulfur composites and additional polymer modification on the carbon surface[23,61].

Plating and stripping of lithium metal in rechargeable lithium batteries is another important example with regards to electrode atom/molecule movement. Owing to the 'hostless' nature of the lithium metal anode and lack of spatial control of lithium deposition, the morphology and structure of electrodes may change continuously during the plating/stripping cycling. Lithium dendrites may grow out of the anode surface upon cycling, which can penetrate the separator and short the battery. If control over the spatial distribution of the redeposited lithium is realized via rational nanostructure design, the main challenges of lithium metal anodes — such as the unstable SEI, low Coulombic efficiency and safety issues — can be solved. As mentioned in 'Solid–electrolyte interphase', a stable artificial interface between lithium metal and the electrolyte, consisting of a monolayer of interconnected hollow carbon nanospheres, was specially designed to achieve a stable SEI and solve the problem of dangerous lithium dendrites (Fig. 3b,c)[15]. Additionally, the use of highly concentrated electrolytes based on ether solvents and lithium bis(fluorosulfonyl)imide salt can enable a compact SEI layer and high-rate cycling of a lithium metal anode without dendrite growth[78].

Besides the sulfur cathode and lithium metal anode, here we would like to emphasize that all the high-capacity electrode materials with large volume change suffer from the problem of atom/molecule diffusion or losses, as it was not specially mentioned in previous literature. Even with a host material, the large volume expansion and structural change of materials and/or electrodes can lead to the diffusion of host atoms or molecules over long distances. Such changes can accumulate and compound on cycling, which may lead to the loss of electrical contact between materials and current collectors, or the detachment of materials from the electrode. The structure change and atom/molecule movement evolve gradually. For conversion oxides, a nanosized mixture of metal (M) and Li_2O is obtained after

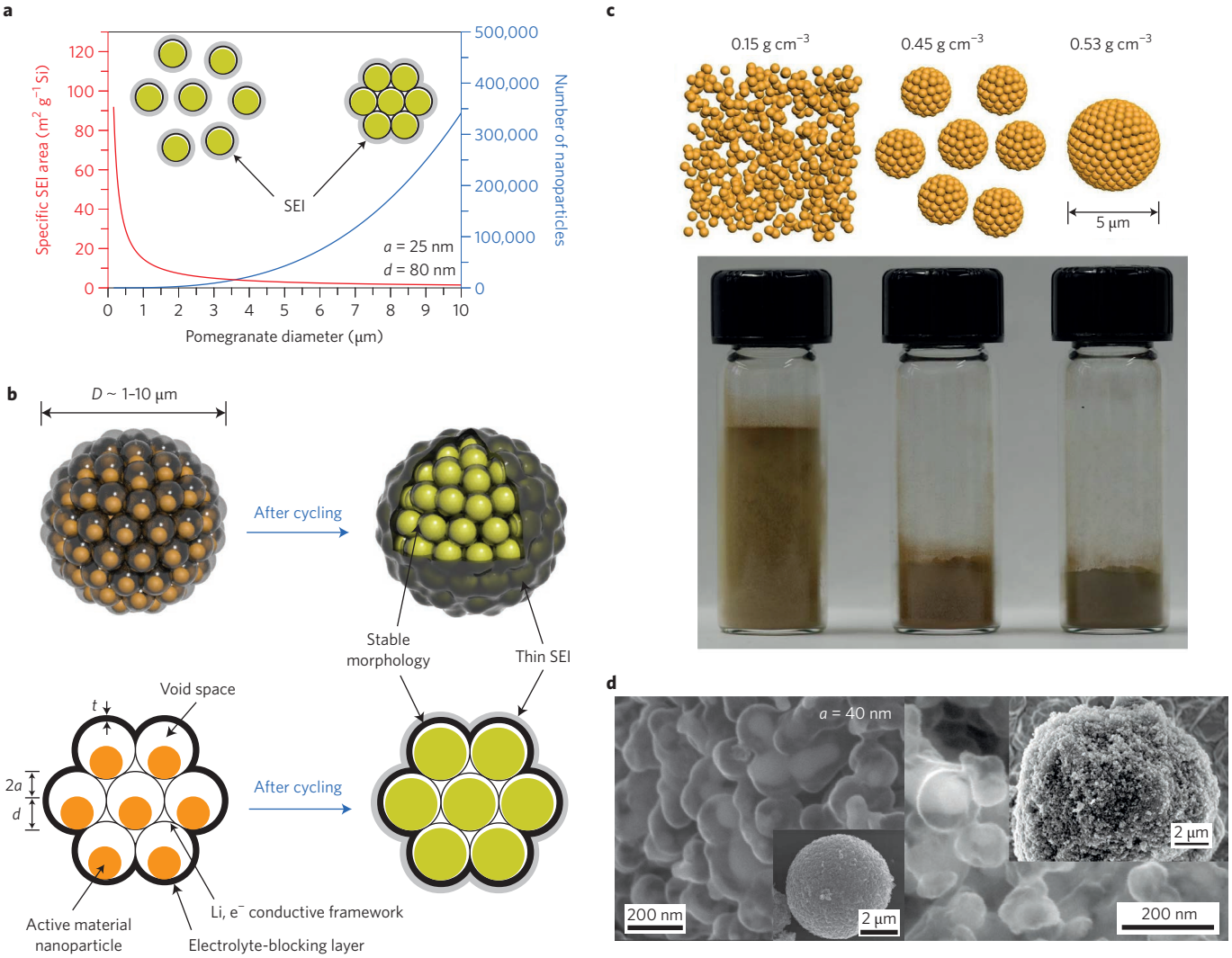

Figure 6 | Solutions for issues of high surface area and low tap density for nanomaterials. a, Calculated surface area in contact with the electrolyte (specific SEI area) for secondary particles composed of primary nanoparticles with the diameter (*d*) of 80 nm, and the number of primary nanoparticles in one secondary particle versus its diameter. *a* is the gap size between primary nanoparticles and their shells. **b**, Schematic of a pomegranate microparticle before and after electrochemical cycling (in the lithiated state). The micrometre size of the secondary particles increases the tap density and decreases the surface area in contact with the electrolyte. The self-supporting conductive carbon framework blocks the electrolyte and prevents SEI formation inside the secondary particle. The well-defined void space around each primary particle allows it to expand without deforming the overall morphology. *D* is the diameter of the secondary particle and *t* is the thickness of the outer shell. **c**, Schematics and pictures of free Si nanoparticles (~80 nm), small secondary particles (~1–2 μm) and large secondary particles (~5 μm) of the same Si nanoparticles. The tap density of the secondary particles is significantly increased. **d**, SEM images of micrometre-sized Si secondary particles prepared via a micro-emulsion approach (pomegranate particle, left) and mechanical approach (right). Figures reproduced from: **a**–**c**,**d** (left panel), ref. 70, NPG; **d** (right panel), ref. 98, RSC.

the initial charge process according to the conversion reaction equation ($M_xO_y + 2yLi^+ + 2ye \rightarrow xM + yLi_2O$), and the overall morphology of the initial particles after the initial cycle can be preserved[17]. However, significant morphology and structure changes may take place after many charge/discharge cycles. For example, marked difference in morphology and structure were observed for a MnO/graphene electrode after 400 discharge/charge cycles[94]. Metal sulfides can transform into nanocomposites of metal and lithium sulfide via a chemical or electrochemical conversion reaction with lithium. The structural and morphological transformations of sulfide nanocrystals (Cu_2S, Co_3S_4 and FeS_2) were investigated by *in situ* high-resolution TEM as they reacted with lithium[43]. The studies revealed that the structure and composition influence the transformation pathway. Similar morphology and structure changes are present in alloy-type materials as well. The surface of Si nanowires and nanotubes becomes very rough and highly porous after 200 cycles, indicating significant material displacement on cycling[68]. The volume-expansion-induced structure changes and the diffusion of atoms/molecules may change the properties of the electrodes, such as conductivity and porosity, which makes it difficult to achieve a long cycle life. Successful examples, which suppress the material solid-state diffusion and realize a long lifespan, include those well-encapsulated nanostructures with void space (for example, Si–SiO_x double-walled silicon nanotubes for 6,000 cycles[68], Si–carbon yolk–shell nanoparticles for 1,000 cycles[69] and Al–TiO_2 yolk–shell nanoparticles for 500 cycles[14]) and crumpled graphene encapsulated particles with self-adaptive strain-relaxation mechanisms (for example, Si/graphene nanoparticles for 200 cycles[95]).

Issues for nanomaterials

The use of nanomaterials may cause many new challenges due to their reduced particle size, such as high surface area, low packing

density and high cost. A rational nanomaterials design must compensate these associated disadvantages while addressing the issues that micrometre-sized materials have. The formation of the SEI layer on the electrode surface consumes the electrolyte and the lithium from the cathode during battery cycling. Compared with electrodes composed of micrometre-scale materials, the SEI formation on the surface of nanostructured electrodes consumes more electrolyte and lithium due to the much higher electrode/electrolyte interfacial area, leading to low initial Coulombic efficiency and significantly reduced overall capacity and energy density of batteries. A stable SEI is critical for the long cycle life of electrodes, while the control of the specific SEI (electrode/electrolyte surface area) plays an important role in achieving high initial Coulombic efficiency.

As discussed above, the issues of large volume expansion and instability of SEI for high-capacity electrode materials are successfully solved by engineering nanostructures with an electrolyte-blocking layer and an internal void space. However, the problem of low initial Coulombic efficiency emerges for these nanostructures owing to their high surface area. High electrode/electrolyte surface area raises the risk of serious side reactions involving electrolyte decomposition and lithium consumption. High surface area is an inherent feature of nanomaterials, but the electrode/electrolyte surface area can be tuned by the engineering of their secondary structures. Figure 6a shows the calculation of specific SEI area for a secondary micrometre-scale particle consisting of assembled nanoparticles. With an electrolyte-blocking layer outside the assembled secondary particles, the specific SEI area can be reduced significantly[70]. Thus, compared with primary nanoparticles, the use of micrometre-scale secondary particles can help to reduce deleterious side reactions between the electrolyte and electrode, and achieve higher initial Coulombic efficiency. Of notable success are Si anode materials with a pomegranate-inspired nanoscale design with the following features (Fig. 6b): micrometre-sized Si secondary particles composed of primary Si nanoparticles; each primary Si nanoparticle has a carbon shell with void space; and each secondary particle has an outer carbon layer as an electrolyte-blocking layer[70]. Besides the reduced specific SEI, fast electron transport pathways are provided by the interconnected carbon framework. The volume expansion of Si on lithiation can be mitigated by the void space. The space-efficient packing of these primary particles also enables high tap density and volumetric mass loading, which are important parameters for electrode evaluations.

Decreasing the particle size to the nanometre scale creates a lot of interparticle space, which usually leads to a low tap density for materials and consequently a low volumetric capacity for an electrode. Nanoparticles tend to bridge/aggregate strongly together into secondary microparticles due to their significantly high surface energy. Besides the interparticle space between secondary microparticles, there is large interparticle space within the aggregation of nanoparticles, leading to higher overall porosity compared with that of the materials with interparticle space between only individual microparticles. Meanwhile, the reduced particle size also induces large interparticle resistance (relative to the same mass loading), which creates barriers for electron transport in the electrode. Thus, it is challenging to achieve electrodes with a high mass loading and areal capacity using nanostructured materials. The tap density of micrometre-sized particles is generally higher than that of free nanoparticles due to the reduced interparticle space. As such, the tap density of nanomaterials can be improved significantly by engineering a micrometre-scale secondary particle/cluster densely assembled by small primary nanoparticles (Fig. 6c)[70]. Two examples among the most successful designs for intercalation-type cathode materials are micrometre-sized $LiNi_{1-x}M_xO_2$ secondary particles composed of aligned needle-like nanosized primary particles[96] and micrometre-scale $LiFePO_4$ secondary particles containing nanoscale carbon-coated primary particles[97]. However, in contrast to these insertion-type cathode materials, engineering the void space for each primary particle is crucial for achieving the long cycle life of high-capacity electrode materials owing to their large volume expansion on lithiation. Based on the aforementioned principles for the secondary cluster design, recently we have shown that high tap density can be achieved for powders composed of micrometre-sized Si secondary particles with a pomegranate-like nanostructure and micrometre-sized Si secondary clusters prepared via a mechanical approach (Fig. 6d)[70,98]. The tap density of the Si secondary clusters fabricated by the mechanical approach is 0.91 g cm^{-3}, six times that of the primary nanoparticles (0.15 g cm^{-3}). Important aspects to note here are that carbon nanotubes are integrated into the Si clusters, which helps to improve intercluster electrical conductivity in the electrode, while within a secondary cluster, the interconnected carbon network provides the pathways for fast electron transport. Thus, owing to the good conductivity, high areal mass loading is achieved for the as-obtained electrodes. As expected, stable cycling with a high areal capacity of ~3.5 mAh cm^{-2} at a high areal mass loading (>2 mg cm^{-2}) is achieved for the as-prepared Si clusters[98]. Therefore, as a result of the space-efficient packing of nanometre-sized primary nanoparticles inside the micrometre-scale secondary particles and the interconnected carbon framework inside each secondary particle, high tap density and mass loading were both achieved. The present strategy of engineering micrometre-scale secondary particles and an interconnected conductive network is both facile and effective for solving the crucial issue of low tap density and mass loading for nanomaterials, and it can be extended to prepare various high-capacity electrode materials.

Although fundamental materials guidelines for designing nanostructrures to improve electrochemical performances have been established, the commercial applications of nanomaterials are still limited by their high cost due to complex synthesis procedures or expensive raw materials. It is crucial to explore facile routes for large-scale synthesis of nanomaterials with low cost. For example, the preparation of Si nanomaterials usually involves expensive processing using high-temperature treatment, high-cost precursors, or equipment set-ups. Recently, progress in low-cost synthesis of porous Si nanomaterials was achieved by means of a magnesiothermic reduction route using highly abundant and low-cost SiO_2 sources, such as silica diatom frustules[99] and rice husks[100]. However, more developments are needed to reduce the cost of nanomaterials in general.

Outlook

In the past decade, various nanostructures have been fabricated to address the significant material and electrode challenges that exist for new battery chemistries. This Review highlights the materials principles used to design these nanostructured materials and gives a broad picture of the developments of nanostructured materials and electrodes that facilitate the advancement of the battery and nanotechnology field. Four major challenges at the material and electrode levels were systematically reviewed, including large volume expansion and fracture, unstable SEI, slow electron/ion transport rate and movements of electrode atoms/molecules. The principles for nanomaterials design in addressing these challenges were discussed in detail and typical examples were provided to illustrate these principles. Meanwhile, new challenges associated with nanomaterials were analysed, including increased specific SEI, reduced tap density and high cost. The understanding and solutions to these new challenges were also discussed.

Future works on understanding the fundamental electrode and materials chemistry taking place in these electrode systems are needed. Detailed information about the electrochemical mechanisms involved in these battery systems is still absent due to their complexity. Meanwhile, investigation of the ion and electron kinetic transport at the electrode/electrolyte interface is also

important, as many electrochemical reactions start at this interface. For example, during the charge and discharge processes, sulfur cathodes undergo numerous phase changes and have various intermediate products. Meanwhile, their electrochemical behaviour in various electrolyte systems is different, and reaction mechanisms related to their electrochemical performance are still not very clear. Further understanding of the Li–S battery chemistry would help to realize an optimized nanostructure design and lead to better electrochemical performance.

New electrode materials involving different battery chemistries and lithium storage mechanisms can offer great improvements in energy density. However, most recent works still focus on improving active material use to achieve high specific capacities with a lower areal capacity than that of existing commercial electrodes. In the future, attention should be paid to improving the mass loading of the electrodes while preserving high active material use. Meanwhile, more intensive research should be devoted to improving the tap density of electrodes composed of high-capacity electrode materials, to improve the volumetric energy density. Approaches that can use close to the high theoretical capacity of active materials, while maintaining high areal mass loading and high tap density of electrodes, are desirable to advance these new rechargeable battery systems far beyond the limit of present lithium-ion batteries.

In addition, the cost of nanomaterial fabrication is normally high. So far, little emphasis has been placed on the low-cost synthesis of high-performance nanostructured electrode materials. For widespread commercial applications, it is of key importance to explore environmentally friendly and facile routes for low-cost large-scale nanomaterials synthesis. Despite the great advances of nanostructure designs to address some major challenges for battery performance, other challenges may still remain beyond the nanostructured electrodes in these new battery systems. Exploration of other interrelated strategies, such as electrolytes, electrolyte additives and new binders, will also help to improve the electrochemical performance of lithium-based rechargeable batteries using nanostructured electrode materials.

Received 3 November 2015; accepted 27 April 2016; published 13 June 2016

References

1. Armand, M. & Tarascon, J.-M. Building better batteries. *Nature* **451,** 652–657 (2008).
2. Goodenough, J. B. & Kim, Y. Challenges for rechargeable Li batteries. *Chem. Mater.* **22,** 587–603 (2010).
3. Dunn, B., Kamath, H. & Tarascon, J.-M. Electrical energy storage for the grid: a battery of choices. *Science* **334,** 928–935 (2011).
4. Scrosati, B. & Garche, J. Lithium batteries: status, prospects and future. *J. Power Sources* **195,** 2419–2430 (2010).
5. Aricò, A. S., Bruce, P., Scrosati, B., Tarascon, J.-M. & van Schalkwijk, W. Nanostructured materials for advanced energy conversion and storage devices. *Nature Mater.* **4,** 366–377 (2005).
6. Li, H., Wang, Z. X., Chen, L. Q. & Huang, X. J. Research on advanced materials for Li-ion batteries. *Adv. Mater.* **21,** 4593–4607 (2009).
7. Bruce, P. G., Freunberger, S. A., Hardwick, L. J. & Tarascon, J.-M. Li–O_2 and Li–S batteries with high energy storage. *Nature Mater.* **11,** 19–29 (2012).
   This paper reviews the development and challenges of Li–O_2 and Li–S batteries, and the fundamental understanding of the related battery chemistry.
8. Chan, C. K. *et al.* High-performance lithium battery anodes using silicon nanowires. *Nature Nanotech.* **3,** 31–35 (2008).
   This paper shows that silicon nanowires as an anode for lithium-ion batteries can accommodate large strain without pulverization, provide good electronic contact and conduction, display short lithium insertion distances, and maintain a high specific capacity during cycling.
9. Magasinski, A. *et al.* High-performance lithium-ion anodes using a hierarchical bottom-up approach. *Nature Mater.* **9,** 353–358 (2010).
10. Kim, H., Han, B., Choo, J. & Cho, J. Three-dimensional porous silicon particles for use in high-performance lithium secondary batteries. *Angew. Chem. Int. Ed.* **47,** 10151–10154 (2008).
11. Derrien, G., Hassoun, J., Panero, S. & Scrosati, B. Nanostructured Sn–C composite as an advanced anode material in high-performance lithium-ion batteries. *Adv. Mater.* **19,** 2336–2340 (2007).
12. Park, C. M. & Sohn, H. J. Black phosphorus and its composite for lithium rechargeable batteries. *Adv. Mater.* **19,** 2465–2468 (2007).
13. Sun, J. *et al.* A phosphorene–graphene hybrid material as a high-capacity anode for sodium-ion batteries. *Nature Nanotech.* **10,** 980–985 (2015).
14. Li, S. *et al.* High-rate aluminium yolk–shell nanoparticle anode for Li-ion battery with long cycle life and ultrahigh capacity. *Nature Commun.* **6,** 7872 (2015).
    This paper demonstrates that a yolk–shell nanostructured aluminium anode, comprising an aluminium core and a TiO_2 shell with tunable interspace, exhibits long cycle life (500 cycles) and reversible capacity of ~1,200 mAh g^{-1} at 1 C.
15. Zheng, G. Y. *et al.* Interconnected hollow carbon nanospheres for stable lithium metal anodes. *Nature Nanotech.* **9,** 618–623 (2014).
    This paper shows that a monolayer of interconnected hollow carbon nanospheres between the lithium metal anode and the electrolyte helps isolate the lithium metal depositions, and facilitates the formation of a stable SEI.
16. Qian, J. F. *et al.* High rate and stable cycling of lithium metal anode. *Nature Commun.* **6,** 6362 (2015).
17. Poizot, P., Laruelle, S., Grugeon, S., Dupont, L. & Tarascon, J.-M. Nano-sized transition-metal oxides as negative-electrode materials for lithium-ion batteries. *Nature* **407,** 496–499 (2000).
    This paper reports that as anode materials for lithium-ion batteries, nanosized transition-metal oxides deliver high specific capacities (~700 mAh g^{-1}) and good capacity retention for up to 100 cycles via an electrochemical conversion reaction mechanism.
18. Kim, Y. & Goodenough, J. B. Lithium insertion into transition-metal monosulfides: tuning the position of the metal 4s band. *J. Phys. Chem. C* **112,** 15060–15064 (2008).
19. Li, H., Richter, G. & Maier, J. Reversible formation and decomposition of LiF clusters using transition metal fluorides as precursors and their application in rechargeable Li batteries. *Adv. Mater.* **15,** 736–739 (2003).
20. Taberna, P. L., Mitra, S., Poizot, P., Simon, P. & Tarascon, J.-M. High rate capabilities Fe_3O_4-based Cu nano-architectured electrodes for lithium-ion battery applications. *Nature Mater.* **5,** 567–573 (2006).
21. Boyanov, S. *et al.* FeP: another attractive anode for the Li-ion battery enlisting a reversible two-step insertion/conversion process. *Chem. Mater.* **18,** 3531–3538 (2006).
22. Fu, Z.-W., Wang, Y., Yue, X.-L., Zhao, S.-L. & Qin, Q.-Z. Electrochemical reactions of lithium with transition metal nitride electrodes. *J. Phys. Chem. B* **108,** 2236–2244 (2004).
23. Ji, X. L., Lee, K. T. & Nazar, L. F. A highly ordered nanostructured carbon–sulphur cathode for lithium–sulphur batteries. *Nature Mater.* **8,** 500–506 (2009).
    This paper reports on the encapsulation of sulfur within the channels of mesoporous carbon and polymer modification of the carbon surfaces, which enables a high reversible capacity for the sulfur cathode of up to 1,320 mAh g^{-1}.
24. Yang, Y. *et al.* Improving the performance of lithium–sulfur batteries by conductive polymer coating. *ACS Nano* **5,** 9187–9193 (2011).
25. Li, W. Y. *et al.* High-performance hollow sulfur nanostructured battery cathode through a scalable, room temperature, one-step, bottom-up approach. *Proc. Natl Acad. Sci. USA* **110,** 7148–7153 (2013).
26. Su, Y.-S. & Manthiram, A. Lithium–sulphur batteries with a microporous carbon paper as a bifunctional interlayer. *Nature Commun.* **3,** 1166 (2012).
27. Suo, L. M., Hu, Y.-S., Li, H., Armand, M. & Chen, L. Q. A new class of Solvent-in-Salt electrolyte for high-energy rechargeable metallic lithium batteries. *Nature Commun.* **4,** 1481 (2013).
28. Peng, Z. Q., Freunberger, S. A., Chen, Y. H. & Bruce, P. G. A reversible and higher-rate Li–O_2 battery. *Science* **337,** 563–566 (2012).
29. Lu, Y. C. *et al.* Platinum–gold nanoparticles: a highly active bifunctional electrocatalyst for rechargeable lithium–air batteries. *J. Am. Chem. Soc.* **132,** 12170–12171 (2010).
30. Aetukuri, N. B. *et al.* Solvating additives drive solution-mediated electrochemistry and enhance toroid growth in non-aqueous Li–O_2 batteries. *Nature Chem.* **7,** 50–56 (2015).
31. Zhou, H.-C., Long, J. R. & Yaghi, O. M. Introduction to metal–organic frameworks. *Chem. Rev.* **112,** 673–674 (2012).
32. Geim, A. K. & Novoselov, K. S. The rise of graphene. *Nature Mater.* **6,** 183–191 (2007).
33. Xia, Y. N. *et al.* One-dimensional nanostructures: synthesis, characterization, and applications. *Adv. Mater.* **15,** 353–389 (2003).
34. Baughman, R. H., Zakhidov, A. A. & de Heer, W. A. Carbon nanotubes—the route toward applications. *Science* **297,** 787–792 (2002).

35. Zhao, D. Y. *et al.* Triblock copolymer syntheses of mesoporous silica with periodic 50 to 300 angstrom pores. *Science* **279,** 548–552 (1998).
36. Alivisatos, A. P. Perspectives on the physical chemistry of semiconductor nanocrystals. *J. Phys. Chem.* **100,** 13226–13239 (1996).
37. Ji, L. W., Lin, Z., Alcoutlabi, M. & Zhang, X. W. Recent developments in nanostructured anode materials for rechargeable lithium-ion batteries. *Energy Environ. Sci.* **4,** 2682–2699 (2011).
38. Bruce, P. G., Scrosati, B. & Tarascon, J.-M. Nanomaterials for rechargeable lithium batteries. *Angew. Chem. Int. Ed.* **47,** 2930–2946 (2008).
39. Winter, M. & Besenhard, J. O. Electrochemical lithiation of tin and tin-based intermetallics and composites. *Electrochim. Acta* **45,** 31–50 (1999).
40. Limthongkul, P., Jang, Y.-I., Dudney, N. J. & Chiang, Y.-M. Electrochemically-driven solid-state amorphization in lithium–silicon alloys and implications for lithium storage. *Acta Mater.* **51,** 1103–1113 (2003).
41. Beaulieu, L. Y., Eberman, K. W., Turner, R. L., Krause, L. J. & Dahn, J. R. Colossal reversible volume changes in lithium alloys. *Electrochem. Solid-State Lett.* **4**, A137–A140 (2001).
42. Lee, S. W., McDowell, M. T., Berla, L. A., Nix, W. D. & Cui, Y. Fracture of crystalline silicon nanopillars during electrochemical lithium insertion. *Proc. Natl Acad. Sci. USA* **109,** 4080–4085 (2012).
43. McDowell, M. T. *et al. In situ* observation of divergent phase transformations in individual sulfide nanocrystals. *Nano Lett.* **15,** 1264–1271 (2015).
44. Maranchi, J. P., Hepp, A. F. & Kumta, P. N. High capacity, reversible silicon thin-film anodes for lithium-ion batteries. *Electrochem. Solid-State Lett.* **6,** A198–A201 (2003).
45. Cheng, Y.-T. & Verbrugge, M. W. The influence of surface mechanics on diffusion induced stresses within spherical nanoparticles. *J. Appl. Phys.* **104,** 083521 (2008).
46. Kalnaus, S., Rhodes, K. & Daniel, C. A study of lithium ion intercalation induced fracture of silicon particles used as anode material in Li-ion battery. *J. Power Sources* **196,** 8116–8124 (2011).
47. McDowell, M. T. *et al.* Studying the kinetics of crystalline silicon nanoparticle lithiation with *in situ* transmission electron microscopy. *Adv. Mater.* **24,** 6034–6041 (2012).
48. Liu, X. H. *et al.* Size-dependent fracture of silicon nanoparticles during lithiation. *ACS Nano* **6,** 1522–1531 (2012).
49. Cui, L.-F., Hu, L. B., Wu, H., Choi, J. W. & Cui, Y. Inorganic glue enabling high performance of silicon particles as lithium ion battery anode. *J. Electrochem. Soc.* **158**, A592–A596 (2011).
50. Kovalenko, I. *et al.* A major constituent of brown algae for use in high-capacity Li-ion batteries. *Science* **334,** 75–79 (2011).
51. Koo, B. *et al.* A highly cross-linked polymeric binder for high-performance silicon negative electrodes in lithium ion batteries. *Angew. Chem. Int. Ed.* **51,** 8762–8767 (2012).
52. Ryou, M.-H. *et al.* Mussel-inspired adhesive binders for high-performance silicon nanoparticle anodes in lithium-ion batteries. *Adv. Mater.* **25,** 1571–1576 (2013).
53. Mao, O. *et al.* Active/inactive nanocomposites as anodes for Li-ion batteries. *Electrochem. Solid-State Lett.* **2,** 3–5 (1999).
54. Kim, I. S., Kumta, P. N. & Blomgren, G. E. Si/TiN nanocomposites novel anode materials for Li-ion batteries. *Electrochem. Solid-State Lett.* **3,** 493–496 (2000).
55. Kim, I. S., Blomgren, G. E. & Kumta, P. N. Si–SiC nanocomposite anodes synthesized using high-energy mechanical milling. *J. Power Sources* **130,** 275–280 (2004).
56. Zheng, W., Liu, Y. W., Hu, X. G. & Zhang, C. F. Novel nanosized adsorbing sulfur composite cathode materials for the advanced secondary lithium batteries. *Electrochim. Acta* **51,** 1330–1335 (2006).
57. Song, M.-S. *et al.* Effects of nanosized adsorbing material on electrochemical properties of sulfur cathodes for Li/S secondary batteries. *J. Electrochem. Soc.* **151,** A791–A795 (2004).
58. Wang, J., Yang, J., Xie, J. & Xu, N. A novel conductive polymer–sulfur composite cathode material for rechargeable lithium batteries. *Adv. Mater.* **14,** 963–965 (2002).
59. Jayaprakash, N., Shen, J., Moganty, S. S., Corona, A. & Archer, L. A. Porous hollow carbon@sulfur composites for high-power lithium–sulfur batteries. *Angew. Chem. Int. Ed.* **50,** 5904–5908 (2011).
60. Li, W. Y. *et al.* Understanding the role of different conductive polymers in improving the nanostructured sulfur cathode performance. *Nano Lett.* **13,** 5534–5540 (2013).
61. Zheng, G. Y. *et al.* Amphiphilic surface modification of hollow carbon nanofibers for improved cycle life of lithium sulfur batteries. *Nano Lett.* **13,** 1265–1270 (2013).
62. Kim, H. *et al.* Plasma-enhanced atomic layer deposition of ultrathin oxide coatings for stabilized lithium–sulfur batteries. *Adv. Energy Mater.* **3,** 1308–1315 (2013).
63. Seh, Z. W. *et al.* Sulphur–TiO_2 yolk–shell nanoarchitecture with internal void space for long-cycle lithium–sulphur batteries. *Nature Commun.* **4,** 1331 (2013).
64. Zhou, W. D., Yu, Y. C., Chen, H., DiSalvo, F. J. & Abruña, H. D. Yolk–shell structure of polyaniline-coated sulfur for lithium–sulfur batteries. *J. Am. Chem. Soc.* **135,** 16736–16743 (2013).
65. Seh, Z. W. *et al.* Two-dimensional layered transition metal disulphides for effective encapsulation of high-capacity lithium sulphide cathodes. *Nature Commun.* **5,** 5017 (2014).
66. Zhang, X. R., Kostecki, R., Richardson, T. J., Pugh, J. K. & Ross, P. N. Jr Electrochemical and infrared studies of the reduction of organic carbonates. *J. Electrochem. Soc.* **148**, A1341–A1345 (2001).
67. Verma, P., Maire, P. & Novák, P. A review of the features and analyses of the solid electrolyte interphase in Li-ion batteries. *Electrochim. Acta* **55,** 6332–6341 (2010).
68. Wu, H. *et al.* Stable cycling of double-walled silicon nanotube battery anodes through solid-electrolyte interphase control. *Nature Nanotech.* **7,** 310–315 (2012).
69. Liu, N. *et al.* A yolk–shell design for stabilized and scalable Li-ion battery alloy anodes. *Nano Lett.* **12,** 3315–3321 (2012).
70. Liu, N. *et al.* A pomegranate-inspired nanoscale design for large-volume-change lithium battery anodes. *Nature Nanotech.* **9,** 187–192 (2014).
This paper demonstrates that a pomegranate-inspired nanostructure for silicon anodes tackles the issues of large volume change, stability of the SEI and low volumetric capacity of nanomaterials, enabling stable cycling and high areal capacity.
71. Wu, H. *et al.* Engineering empty space between Si nanoparticles for lithium-ion battery anodes. *Nano Lett.* **12,** 904–909 (2012).
72. Zhang, W. M. *et al.* Tin-nanoparticles encapsulated in elastic hollow carbon spheres for high-performance anode material in lithium-ion batteries. *Adv. Mater.* **20,** 1160–1165 (2008).
73. Zhang, H. W. *et al.* Tailoring the void size of iron oxide@carbon yolk–shell structure for optimized lithium storage. *Adv. Funct. Mater.* **24,** 4337–4342 (2014).
74. Xu, K. Nonaqueous liquid electrolytes for lithium-based rechargeable batteries. *Chem. Rev.* **104,** 4303–4417 (2004).
75. Yan, K. *et al.* Ultrathin two-dimensional atomic crystals as stable interfacial layer for improvement of lithium metal anode. *Nano Lett.* **14,** 6016–6022 (2014).
76. Kozen, A. C. *et al.* Next-generation lithium metal anode engineering via atomic layer deposition. *ACS Nano* **9,** 5884–5892 (2015).
77. Li, N.-W., Yin, Y.-X., Yang, C.-P. & Guo, Y.-G. An artificial solid electrolyte interphase layer for stable lithium metal anodes. *Adv. Mater.* **28,** 1853–1858 (2015).
78. Li, W. Y. *et al.* The synergetic effect of lithium polysulfide and lithium nitrate to prevent lithium dendrite growth. *Nature Commun.* **6,** 7436 (2015).
79. Hwang, T. H., Lee, Y. M., Kong, B.-S., Seo, J.-S. & Choi, J. W. Electrospun core–shell fibers for robust silicon nanoparticle-based lithium ion battery anodes. *Nano Lett.* **12,** 802–807 (2012).
80. Xu, Y. H. *et al.* Uniform nano-Sn/C composite anodes for lithium ion batteries. *Nano Lett.* **13,** 470–474 (2013).
81. Li, Y. G., Tan, B. & Wu, Y. Y. Mesoporous Co_3O_4 nanowire arrays for lithium ion batteries with high capacity and rate capability. *Nano Lett.* **8,** 265–270 (2008).
82. Yao, Y. *et al.* Interconnected silicon hollow nanospheres for lithium-ion battery anodes with long cycle life. *Nano Lett.* **11,** 2949–2954 (2011).
83. Liang, Z. *et al.* Sulfur cathodes with hydrogen reduced titanium dioxide inverse opal structure. *ACS Nano* **8,** 5249–5256 (2014).
84. Cao, F. F. *et al.* Cu–Si nanocable arrays as high-rate anode materials for lithium-ion batteries. *Adv. Mater.* **23,** 4415–4420 (2011).
85. Hu, L. B. *et al.* Silicon–carbon nanotube coaxial sponge as Li-ion anodes with high areal capacity. *Adv. Energy Mater.* **1,** 523–527 (2011).
86. Wei, W. *et al.* 3D graphene foams cross-linked with pre-encapsulated Fe_3O_4 nanospheres for enhanced lithium storage. *Adv. Mater.* **25,** 2909–2914 (2013).
87. Chan, C. K., Zhang, X. F. & Cui, Y. High capacity Li ion battery anodes using Ge nanowires. *Nano Lett.* **8,** 307–309 (2008).
88. Yang, C.-P., Yin, Y.-X., Zhang, S.-F., Li, N.-W. & Guo, Y.-G., Accommodating lithium into 3D current collectors with a submicron skeleton towards long-life lithium metal anodes. *Nature Commun.* **6,** 8058 (2015).
This paper reports that a 3D Cu current collector with a submicron skeleton and high electroactive surface area can significantly improve the electrochemical deposition behaviour of Li, including suppression of the growth of Li dendrites, low voltage hysteresis and long lifespan.
89. Zhang, R. *et al.* Conductive nanostructured scaffolds render low local current density to inhibit lithium dendrite growth. *Adv. Mater.* **28,** 2155–2162 (2016).
90. Yamin, H. & Peled, E. Electrochemistry of a nonaqueous lithium/sulfur cell. *J. Power Sources* **9,** 281–287 (1983).
91. Elazari, R. *et al.* Morphological and structural studies of composite sulfur electrodes upon cycling by HRTEM, AFM and Raman spectroscopy. *J. Electrochem. Soc.* **157,** A1131–A1138 (2010).

92. Yao, H. B. *et al.* Improving lithium–sulphur batteries through spatial control of sulphur species deposition on a hybrid electrode surface. *Nature Commun.* **5,** 3943 (2014).
93. Pang, Q., Kundu, D., Cuisinier, M. & Nazar, L. F. Surface-enhanced redox chemistry of polysulphides on a metallic and polar host for lithium–sulphur batteries. *Nature Commun.* **5,** 4759 (2014).
94. Sun, Y. M., Hu, X. L., Luo, W., Xia, F. F. & Huang, Y. H. Reconstruction of conformal nanoscale MnO on graphene as a high-capacity and long-life anode material for lithium ion batteries. *Adv. Funct. Mater.* **23,** 2436–2444 (2012).
95. Son, I. H. *et al.* Silicon carbide-free graphene growth on silicon for lithium-ion battery with high volumetric energy density. *Nature Commun.* **6,** 7393 (2015).
96. Sun, Y.-K. *et al.* Nanostructured high-energy cathode materials for advanced lithium batteries. *Nature Mater.* **11,** 942–947 (2012).
97. Oh, S. W. *et al.* Double carbon coating of $LiFePO_4$ as high rate electrode for rechargeable lithium batteries. *Adv. Mater.* **22,** 4842–4845 (2010).
98. Lin, D. C. *et al.* A high tap density secondary silicon particle anode fabricated by scalable mechanical pressing for lithium-ion batteries. *Energy Environ. Sci.* **8,** 2371–2376 (2015).
99. Bao, Z. *et al.* Chemical reduction of three-dimensional silica micro-assemblies into microporous silicon replicas. *Nature* **446,** 172–175 (2007).
100. Liu, N., Huo, K. F., McDowell, M. T., Zhao, J. & Cui, Y. Rice husks as a sustainable source of nanostructured silicon for high performance Li-ion battery anodes. *Sci. Rep.* **3,** 1919 (2013).

Acknowledgements

Y.C. acknowledges the support from the Assistant Secretary for Energy Efficiency and Renewable Energy, Office of Vehicle Technologies of the US Department of Energy under the Battery Materials Research (BMR) Program, and the support from the Joint Center for Energy Storage Research (JCESR), an Energy Innovation Hub funded by the US Department of Energy, Office of Science, Basic Energy Sciences.

Additional information

Reprints and permissions information is available online at www.nature.com/reprints. Correspondence should be addressed to Y.C.

Competing interests

The authors declare no competing financial interests.